Photochemical & Photobiological Sciences

PERSPECTIVE

View Article Online
View Journal

Cite this: DOI: 10.1039/c9pp00400a

Recent advances in studies on the magneto-chiral dichroism of organic compounds

Kazuyuki Ishii, * Shingo Hattori and Yuichi Kitagawa

Magneto-chiral dichroism (MChD) is an interesting phenomenon in which the absorbance of a chiral molecule depends on the direction of the magnetic field. As the MChD of two enantiomers is opposite in nature, MChD has received considerable attention for the development of magneto-optical devices and new asymmetric synthetic methods, as well as being an explanation for the origin of the homochirality of life. In this perspective, the theoretical background behind MChD is introduced, and then, the first examples of metal complexes and aromatic π-conjugated systems are discussed. Furthermore, the electronic properties of aromatic π-conjugated systems, such as orbital angular momentum and exciton chirality, are theoretically explained, and the possibility of MChD-based photoresolutions is described.

Received 30th September 2019,
Accepted 15th November 2019

DOI: 10.1039/c9pp00400a

rsc.li/pps

Introduction

Magneto-chiral dichroism (MChD) is a magneto-optical effect in which the absorption coefficient of a chiral molecule in an unpolarised light beam changes depending on whether an externally applied magnetic field is parallel or antiparallel to the direction of light propagation (Fig. 1).[1,2] As the MChD of two enantiomers is opposite in nature, this phenomenon is of great interest, receiving considerable attention for the development of novel magneto-optical devices and new asymmetric synthetic methods. MChD is also a possible explanation for the origin of the homochirality of life.[3–16]

Early research on MChD had purely theoretical roots. Wagnière and Meier first calculated the magnetically induced changes for the absorption and emission rates of chiral molecules.[1] Based on these results and molecular theory, Barron and Vrbancich later showed that the absorption coefficient of a chiral system exposed to unpolarised light is different when an externally applied magnetic field is parallel or antiparallel to the direction of light propagation, in addition to magneto-chiral birefringence.[2,3] This difference occurs even for un-

Institute of Industrial Science, The University of Tokyo, Komaba, Meguro-ku, Tokyo 153-8505, Japan. E-mail: k-ishii@iis.u-tokyo.ac.jp

Kazuyuki Ishii

Kazuyuki Ishii received his Ph.D. in 1996 from Tohoku University under the supervision of Prof. Seigo Yamauchi, and subsequently worked as a research associate in the laboratory of Prof. Nagao Kobayashi (April 1996–March 2006, Tohoku University). He is currently a full Professor at the Institute of Industrial Science of The University of Tokyo. His interests include homochirality of life, photodynamic therapy, fluorescence bioimaging, time-resolved ESR spectroscopy, and chiroptical spectroscopy.

Shingo Hattori

Shingo Hattori earned his Ph.D. in chemistry from The University of Tokyo in 2017 under the direction of Professor Kazuyuki Ishii. He worked as a postdoctoral researcher in the laboratory of Professor Kazuyuki Ishii at The University of Tokyo from 2017 to 2019. Since 2019, he has been an assistant professor at Yokohama City University. His interests include photochemistry of organic chiral compounds and metal complexes.

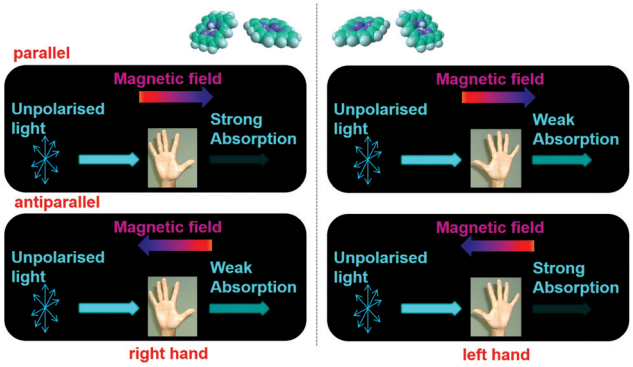

Fig. 1 Illustration of MChD as a magneto-optical effect. The absorption coefficient of a chiral molecule is different for an unpolarised light beam when an externally applied magnetic field is parallel or antiparallel to the direction of light propagation. The MChD effects of two enantiomers are opposite.

polarised light, and it is opposite for two enantiomers. Compounds that exhibit both strong circular dichroism (CD) and magnetic circular dichroism (MCD) are expected to show MChD. Although CD and MCD effects are seemingly linked, the origins of CD and MCD, which are molecular chirality and orbital angular momentum, respectively, are completely different.

Following these theoretical predictions, MChD was experimentally confirmed for the first time in the $^5D_0 \rightarrow {}^7F_{1,2}$ luminescent transition of a europium(III) complex.[4] MChD observations have subsequently been reported for inorganic compounds containing transition metal or lanthanide ions, π–π* transitions in organic compounds, and photoresolution based on MChD. Even 20 years after the first observation of MChD, reports on MChD observations have been limited due to both its weak manifestation arising from the cross effect of CD and MCD and the lack of conventional measurement systems. However, despite its challenges, MChD has attracted considerable attention due to the interplay between chirality and magnetism, resulting in the development of not only novel materials but also measurement systems using various electromagnetic waves. The observation of MChD in compounds related to living beings has further led to studies to explore the relationship between MChD and living systems, such as understanding the origin of the homochirality of life.

In this perspective, we describe the recent progress of MChD focusing on organic compounds. In the "Theoretical background" section, the basic theory of MChD is described for readers to understand the principles of MChD. In the "Magneto-chiral dichroism of metal compounds" section, historically representative MChD observations are introduced. In the "Magneto-chiral dichroism of aromatic π-conjugated systems" section, MChD observations of aromatic π-conjugated systems are illustrated, with the origin of the MChD intensity theoretically described in detail. In the "Photoresolution based on magneto-chiral dichroism" section, enantioselective photochemical reactions are introduced in metal complexes and organic polymers. Finally, future directions are described in terms of asymmetric synthesis and provide a clue to the homochirality of life.

Theoretical background

The MChD intensity in isotropic media is expressed as follows.[2,3]

$$\eta^{\uparrow\uparrow} - \eta^{\uparrow\downarrow} \approx \frac{2\mu_0 c N_0 B_z}{3\hbar}\left[\left\{\frac{2({\omega_{na}}^2+\omega^2)}{\hbar} fgA(G) - \frac{4\omega_{na}\omega}{\hbar} fgA(A')\right\} + \left\{\omega_{na} g\left(B(G)+\frac{C(G)}{kT}\right) - \omega g\left(B(A')+\frac{C(A')}{kT}\right)\right\}\right] \quad (1)$$

$$f = \frac{{\omega_{na}}^2 - \omega^2}{({\omega_{na}}^2 - \omega^2) + \omega^2 {\Gamma_{na}}^2} \quad (2)$$

$$g = \frac{\omega \Gamma_{na}}{({\omega_{na}}^2 - \omega^2) + \omega^2 {\Gamma_{na}}^2} \quad (3)$$

where N_0 is the number density, μ_0 is the vacuum permeability, and c is the velocity of light in a vacuum. For a transition between the ground state, a, and the excited state, n, the variables f and g represent the dispersion-type and integral-type line shape functions, respectively; ω_{na} and Γ_{na} correspond to the angular frequency of the transition energy and the full bandwidth at half maximum, respectively.

MChD effects can be classified into three general terms referred to as the A-term, B-term, and C-term, which depend on the degenerate states and should not be confused with spin sublevel degeneracy. Each general term can be further classified with G or A', ultimately leading to six possible terms. The

Yuichi Kitagawa

Yuichi Kitagawa obtained his Ph.D. (2012) from the School of Engineering, University of Tokyo. He was a research fellow of the Japan Society for the Promotion of Science (JSPS) (2013) at Ritsumeikan University. He was an assistant professor (2014–2018) at Hokkaido University. Since 2019 he has been a lecturer at Hokkaido University. His interests are molecular photophysics and photochemistry. He is now studying the luminescence, chiroptical, and magneto-optical properties of lanthanide(III) complexes.

magneto-chiral A-terms, $A(G)$ and $A(A')$, are observed for degenerate electronic states arising from the Zeeman effect, while the magneto-chiral B-terms, $B(G)$ and $B(A')$, are observed for nondegenerate electronic states that interact with each other *via* magnetic dipole moments. The magneto-chiral C-terms, $C(G)$ and $C(A')$, are temperature-dependent due to the change in the Boltzmann distribution. These six terms are expressed by the following equations:

$$A(G) = \varepsilon_{\alpha\beta\gamma}\frac{1}{d_a}\sum_a (m_{n\gamma} - m_{a\gamma})\mathrm{Re}(\langle\varphi_a|\mu_\alpha|\varphi_n\rangle\langle\varphi_n|m_\beta|\varphi_a\rangle) \quad (4)$$

$$A(A') = \frac{\omega}{15d_a}\sum_a (m_{n\beta} - m_{a\beta})\mathrm{Im}(3\langle\varphi_a|\mu_\alpha|\varphi_n\rangle\langle\varphi_n|\Theta_{\alpha\beta}|\varphi_a\rangle - \langle\varphi_a|\mu_\beta|\varphi_n\rangle\langle\varphi_n|\Theta_{\alpha\alpha}|\varphi_a\rangle) \quad (5)$$

$$\begin{aligned} B(G) = \varepsilon_{\alpha\beta\gamma}\frac{1}{d_a}\sum_a \mathrm{Re}\Bigg\{ & \sum_{m\neq a}\frac{\langle\varphi_m|m_\gamma|\varphi_a\rangle}{E_m - E_a}\big(\langle\varphi_a|\mu_\alpha|\varphi_n\rangle\langle\varphi_n|m_\beta|\varphi_m\rangle \\ & + \langle\varphi_a|m_\beta|\varphi_n\rangle\langle\varphi_n|\mu_\alpha|\varphi_m\rangle\big) \\ & + \sum_{m\neq n}\frac{\langle\varphi_n|m_\gamma|\varphi_m\rangle}{E_m - E_n}\big(\langle\varphi_a|\mu_\alpha|\varphi_n\rangle\langle\varphi_m|m_\beta|\varphi_a\rangle \\ & + \langle\varphi_a|m_\beta|\varphi_n\rangle\langle\varphi_m|\mu_\alpha|\varphi_a\rangle\big)\Bigg\} \end{aligned} \quad (6)$$

$$\begin{aligned} B(A') = \frac{\omega}{15d_a}\sum_a \mathrm{Im}\Bigg\{ & \sum_{m\neq a}\frac{\langle\varphi_m|m_\beta|\varphi_a\rangle}{E_m - E_a}(3(\langle\varphi_a|\mu_\alpha|\varphi_n\rangle\langle\varphi_n|\Theta_{\alpha\beta}|\varphi_m\rangle \\ & -\langle\varphi_a|\Theta_{\alpha\beta}|\varphi_n\rangle\langle\varphi_n|\mu_\alpha|\varphi_m\rangle) - (\langle\varphi_a|\mu_\beta|\varphi_n\rangle\langle\varphi_n|\Theta_{\alpha\alpha}|\varphi_m\rangle \\ & -\langle\varphi_a|\Theta_{\alpha\alpha}|\varphi_n\rangle\langle\varphi_n|\mu_\beta|\varphi_m\rangle)) \\ & + \sum_{m\neq n}\frac{\langle\varphi_n|m_\beta|\varphi_m\rangle}{E_m - E_n}(3(\langle\varphi_a|\mu_\alpha|\varphi_n\rangle\langle\varphi_m|\Theta_{\alpha\beta}|\varphi_a\rangle \\ & -\langle\varphi_a|\Theta_{\alpha\beta}|\varphi_n\rangle\langle\varphi_m|\mu_\alpha|\varphi_a\rangle) - (\langle\varphi_a|\mu_\beta|\varphi_n\rangle\langle\varphi_m|\Theta_{\alpha\alpha}|\varphi_a\rangle \\ & -\langle\varphi_a|\Theta_{\alpha\alpha}|\varphi_n\rangle\langle\varphi_m|\mu_\beta|\varphi_a\rangle))\Bigg\} \end{aligned} \quad (7)$$

$$C(G) = \varepsilon_{\alpha\beta\gamma}\frac{1}{d_a}\sum_a m_{a\gamma}\mathrm{Re}(\langle\varphi_a|\mu_\alpha|\varphi_n\rangle\langle\varphi_n|m_\beta|\varphi_a\rangle) \quad (8)$$

$$C(A') = \frac{\omega}{15d_a}\sum_a m_{a\beta}\mathrm{Im}(3\langle\varphi_a|\mu_\alpha|\varphi_n\rangle\langle\varphi_n|\Theta_{\alpha\beta}|\varphi_a\rangle - \langle\varphi_a|\mu_\beta|\varphi_n\rangle\langle\varphi_n|\Theta_{\alpha\alpha}|\varphi_a\rangle) \quad (9)$$

where ψ_i and E_i are the wavefunction and energy of the i state, respectively ($i = a$, m, or n), d_a represents the degeneracy of the ground state, and $\varepsilon_{\alpha\beta\gamma}$ denotes the alternating tensor (Levi-Civita). The electric dipole (μ_α), magnetic dipole (m_α), and electric quadrupole ($\Theta_{\alpha\alpha}$) operators are expressed as follows:

$$\mu_\alpha = \sum_i e_i r_{i\alpha} \quad (10)$$

$$m_\alpha = \sum_i \frac{e}{2m}\varepsilon_{\alpha\beta\gamma} r_{i\beta} p_{i\gamma} \quad (11)$$

$$\Theta_{\alpha\beta} = \frac{1}{2}\sum_i e_i(3r_{i\alpha}r_{i\beta} - {r_i}^2\delta_{\alpha\beta}) \quad (12)$$

where e and m denote the charge and mass of an electron, respectively, $r_{i\alpha}$ is the position operator, and p_{ir} is the momentum operator. When the terms related to $1/(E_m - E_a)$ are negligible because of the large excitation energy, the MChD intensity therefore corresponds to the electric dipole, magnetic dipole, and electric quadrupole moments for the transition between the a and n (or m) states in addition to the magnetic dipole moments between n and m states.

The matrix elements resulting in CD and MCD intensities are similar to those for the MChD intensity.[5,6] The CD intensity corresponds to an imaginary part of the scalar product of the electric dipole and magnetic dipole moments for the transition between the a and n states; only chiral molecules exhibit CD.

$$R = \mathrm{Im}\{\langle\varphi_\mathrm{a}|\mu|\varphi_n\rangle\cdot\langle\varphi_n|m|\varphi_\mathrm{a}\rangle\} \quad (13)$$

Furthermore, the MCD intensity corresponds to the transition electric dipole moment between the a and n states and the magnetic dipole moment between the n and m states; MCD is a property of all matter.

$$\Delta\eta = \frac{-\mu_0 c l N_0 B_\mathrm{Z}}{3\hbar}\left\{\frac{4\omega_{na}\omega^2}{\hbar}(fg)A + \omega^2 g\left(B + \frac{C}{kT}\right)\right\} \quad (14)$$

$$A = \frac{1}{2d_a}(m_n - m_a)\mathrm{Im}(\langle\varphi_a|\mu|\varphi_n\rangle\langle\varphi_n|\mu|\varphi_a\rangle) \quad (15)$$

$$B = \frac{1}{d_a}\mathrm{Im}\left(\sum_{m\neq a}\frac{\langle\varphi_m|m|\varphi_a\rangle}{E_m - E_a}\langle\varphi_a|\mu|\varphi_n\rangle\langle\varphi_n|\mu|\varphi_m\rangle + \sum_{m\neq n}\frac{\langle\varphi_n|m|\varphi_m\rangle}{E_m - E_n}\langle\varphi_a|\mu|\varphi_n\rangle\langle\varphi_m|\mu|\varphi_a\rangle\right) \quad (16)$$

$$C = \frac{1}{2d_a}m_a\mathrm{Im}(\langle\varphi_a|\mu|\varphi_n\rangle\langle\varphi_n|\mu|\varphi_a\rangle) \quad (17)$$

Since the matrix elements for the CD and MCD intensities are similar to those for the MChD intensity,[5,6] the following equation can only be used when the MCD spectrum is dominated by the Faraday A-term.[5]

$$g_\mathrm{MChD} \approx g_\mathrm{CD} \times g_\mathrm{MCD} \quad (18)$$

Here, the g values, g_MChD, g_CD and g_MCD, indicate the ratio of the absorption difference and the total absorption. MChD is a cross effect between the CD and MCD effects, and therefore, the magnitude of g_MChD can be roughly estimated from the product of g_CD and g_MCD.[5] Thus, MChD is expected to be experimentally observed for chiral compounds that show both strong CD and MCD, and would be weak.

Magneto-chiral dichroism of metal compounds

After theoretical predictions were made, Rikken and Raupach reported the first experimental MChD observations in the $^5D_0 \rightarrow {}^7F_{1,2}$ luminescence of chiral europium(III) tris(3-trifluoroace-

tyl-±-camphorato), Eu((±)tfc)$_3$.[4] Fig. 2 shows the MChD spectra for both enantiomers of the Eu^{3+} complex. The large orbital angular momentum of the f orbitals has a pronounced effect on MChD, with the Eu^{3+} complex exhibiting considerable MCD in the f–f transitions.[17] The unpolarised luminescence intensity changes when an externally applied magnetic field is switched between being parallel and antiparallel to the direction of light propagation. A phase-sensitive detection method and alternating magnetic field directions were employed in order to increase the signal-to-noise ratio. The $^5D_0 \rightarrow {}^7F_1$ and $^5D_0 \rightarrow {}^7F_2$ transitions produced MChD signals that were opposite in sign for the two enantiomers. Moreover, the MChD intensity is proportional to the magnetic field strength (inset of Fig. 2). For the $^5D_0 \rightarrow {}^7F_1$ transition, the experimental g_{MChD} value (5×10^{-3}) is ~10 times greater than the $g_{CD} \times g_{MCD}$ cross product (4×10^{-4}).[5,6]

Rikken and co-workers investigated the MChD effects of chiral uniaxial crystals of α-$NiSO_4 \cdot 6H_2O$,[5] which exhibited intense CD and MCD signals.[18,19] It was confirmed that MChD was uninfluenced not only by light intensity, but also by reversing the crystals towards the direction of light propagation. The intensity calculated based on the Baranova model is consistent with the observed intensity, but the calculated and observed spectra differ significantly. The possibilities of cascaded MChD were also investigated in this system. When unpolarised light penetrates optically active materials, it becomes circularly polarised light (CPL). Since a magnetic field induces MCD effects in this case, the transmitted light intensity depends on the relationship between the direction of light propagation and the magnetic field direction. This is referred to as cascaded MChD, and it essentially appears as pure MChD. Pure MChD can be distinguished from cascaded MChD by examining concentration dependencies. When the optical path lengths are fixed, pure MChD is linearly proportional to the concentration of MChD-active species. On the other hand, cascaded MChD is proportional to the square of the concentration of the active species because it is proportional to the product of the concentration of CD-active and MCD-active species. By comparing the cascaded MChD spectrum with the MChD spectra of α-$NiSO_4 \cdot 6H_2O$ at different concentrations, a pure MChD effect can be identified. Rikken and coworkers also developed a multichannel MChD spectrometer, in which the optical properties of the sample are modulated by an alternating external magnetic field. By using this spectrometer, MChD of α-$NiSO_4 \cdot 6H_2O$ crystals was examined.[20]

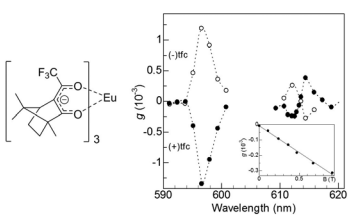

Fig. 2 A molecular structure of tris(3-trifluoroacetyl-±-camphorato) europium(III) (left) and magneto-chiral luminescence anisotropy of Eu((±)tfc)$_3$ complexes in deuterated dimethyl sulfoxide (right). The inset shows a magnetic field dependence of the magneto-chiral anisotropy (λ_{ex} = 350 nm, λ_{em} = 615.8 nm). Reproduced from ref. 4 with permission from Springer Nature.

Various materials have been investigated in order to enhance MChD. Train *et al.* reported the first observation of MChD in an enantiopure, chiral ferromagnet using chromium–manganese two-dimensional oxalate layers.[8] The MChD intensity was enhanced by a factor of 17 in the ferromagnetic phase. Arima and co-workers reported the very intense MChD effects of CuB_2O_4, which exhibited magnetically induced chirality.[9] The observed MChD was approximately 10^4 times greater than that observed previously for paramagnetic molecules. They also investigated the MChD of right- and left-handed $CsCuCl_3$ crystals in strong magnetic fields (up to 14.5 T), identifying a change in the absorption coefficient from the d–d transition of intra-atomic Cu^{2+} ions.[21] Rikken and co-workers investigated chiral magnetic nanohelices with critical dimensions comparable to the ferromagnetic domain size.[22] A chiral Ni^{2+} film consisting of an array of nanohelices ~100 nm in length exhibited a MChD anisotropy factor (g_{MChD}) of ~10^{-4} T^{-1} at room temperature, which is the first report on MChD in a material with structural chirality on the order of the wavelength of light. Taniguchi *et al.* demonstrated strong MChD for visible light emission using a chiral Tb^{3+} complex, in which the MChD luminescence signal reaches ~16% at 14 T.[23] They also investigated heterometallic systems with short-range correlations (*e.g.*, cyano-bridged copper(II)–chromium(III) coordination polymers) and demonstrated that MChD in d–d transitions of Cu^{2+} coordinated to chiral ligands, which is mainly proportional to the magnetisation of the local Cu^{2+} centre.[24] Yannopapas *et al.* theoretically investigated magnetic nanoparticle helices coiled around plasmonic gold nanorods, calculating very strong MChD for this system.[25,26]

In addition to the UV-vis-NIR region, MChD effects have also been investigated in the X-ray region. Ceolín investigated the hard X-ray absorption spectra of $\{Tb[Ni(pro)_2]_6\}^{3+}$ (pro = L- or D-prolinate), discovering a large MChD (1%) at room temperature.[27] Sessoli and co-workers investigated the element selective hard X-ray MChD of enantiopure crystals of two isostructural molecular helicoidal chains comprising either Co^{2+} or Mn^{2+} ions.[28] A strong MChD (>3%) was observed in the cobalt chain system, whereas it was practically absent for the manganese derivative.

In the THz and GHz regions, Tokura and co-workers investigated the MChD phenomena based on spin excitation using $Ba_2CoGe_2O_7$, a square-lattice antiferromagnet that undergoes a magnetic field driven transition to a chiral form.[29] Complete MChD (~100%) in the THz region occurs as a result of spin excitation. They also investigated the MChD of multiferroic materials, such as $CuFe_{1-x}Ga_xO_2$ (x = 0.035), $Ba_3NbFe_3Si_2O_{14}$, $MnWO_4$, and Cu_2OSeO_3. The collective spin excitations active for both electric and magnetic fields are referred to as electro-

magnons; the electromagnon resonance for the screw spin helimagnet $CuFe_{1-x}Ga_xO_2$ (x = 0.035) exhibited a very large MChD effect (400%).[30–33] Ueda and co-workers investigated the MChD of a metamaterial consisting of a chiral copper structure and ferrite rod, determining the directional differences of X-band microwaves to be 10^{-3} at 200 mT.[34,35] Microwave MChD was observed in the non-centrosymmetric magnet CuB_2O_4 by Nii *et al.*[36]

Magneto-chiral dichroism of aromatic π-conjugated systems

Magneto-chiral dichroism of organic compounds

As described in the previous section, several MChD observations have been reported for inorganic compounds.[4–9,20–36] This is a retrospectively reasonable finding, since MCD, a significant contributor to MChD, is intensified by the d (or f) orbital-based degeneracy and angular momentum of metals. This advantage does not exist for organic compounds, making the MChD of organic compounds associated with living beings more difficult to establish; a revelatory research effort identified that the orbital angular momentum of organic aromatic compounds helps overcome this challenge. The magnitude of orbital angular momentum corresponds to the magnetic quantum number, m_l. The π molecular orbitals of organic aromatic compounds are quantised by m_l (similar to atomic orbitals), and the maximum $|m_l|$ values of the π molecular orbitals of organic aromatic compounds increase with an increase in the size of π-conjugated systems, as described in detail in the "Theoretical explanations for magneto-chiral dichroism of aromatic π-conjugated systems" section.[37,38]

Ishii and co-workers attempted to observe the first MChD of organic compounds associated with living beings.[10] To achieve this, the chiral J-aggregates of water-soluble tetraarylporphyrins were employed. Porphyrin molecules possess a large aromatic π-conjugated system with a large orbital angular momentum, resulting in intense MCD signals. Moreover, a very intense CD signal is obtained by exploiting the exciton chirality that exists within the twisted configurations between porphyrin constituents.[39,40] Fig. 3 shows the UV-vis, CD, and MCD spectra of the protonated forms of *meso*-tetrakis(4-sulfonatophenyl)porphine (H_4TPPS_4, Fig. 3a) and the chiral J-aggregates of H_4TPPS_4 (Fig. 3b). The chiral J-aggregates were prepared by adding chiral tartaric acid, which induces Coulomb interactions between the positively charged protonated pyrroles and the negatively charged sulfonate groups.[10,41,42] Formation of the J-aggregates causes a considerable bathochromic shift of the Soret band (π–π* transition) to

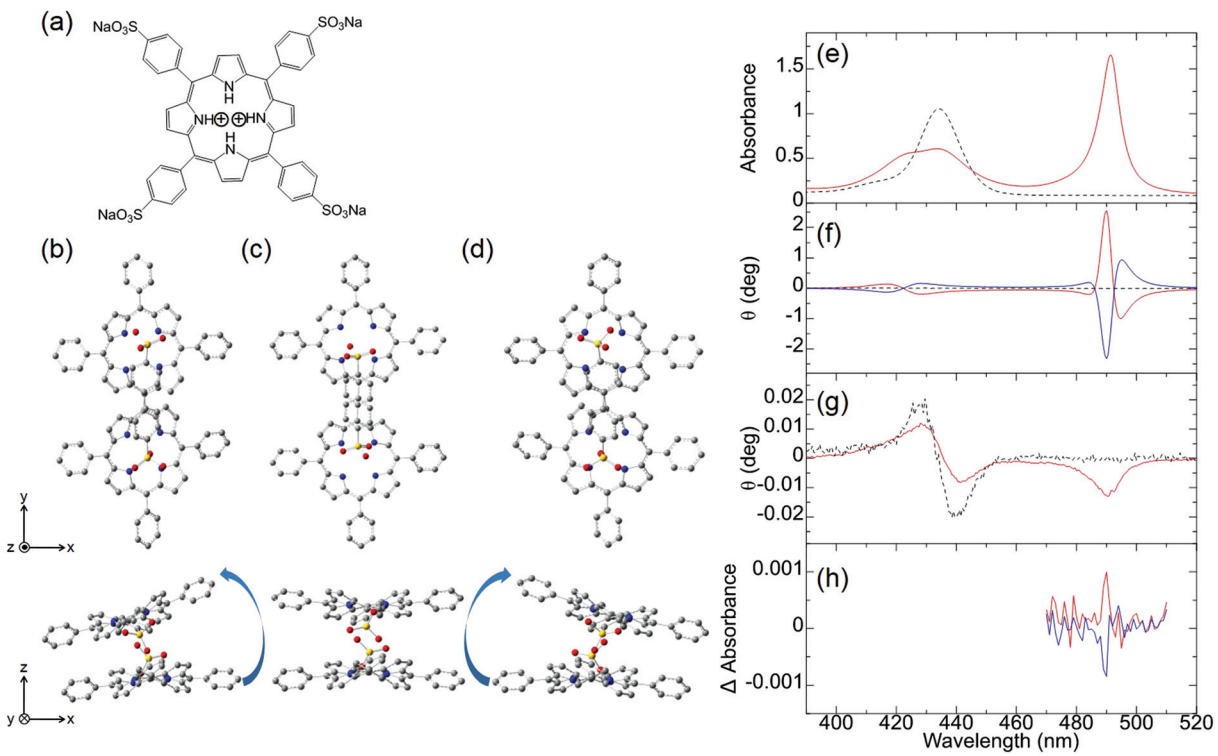

Fig. 3 H_4TPPS_4 and chiral J-aggregates of H_4TPPS_4. (a) The molecular structure of H_4TPPS_4 and optimised H_4TPPS_1 dimer configurations as (b) left-handed helical, (c) parallel, and (d) right-handed helical structures. The (e) UV-vis, (f) CD, (g) MCD, and (h) MChD spectra of H_4TPPS_4 (black broken lines) and the chiral J-aggregates of H_4TPPS_4 (solid lines). The chiral J-aggregates of H_4TPPS_4 were prepared by the addition of L-tartaric acid (red solid line) or D-tartaric acid (blue solid line). Reproduced from ref. 10 with permission from John Wiley and Sons.

490 nm owing to the exciton interactions between the H_4TPPS_4 constituents (Fig. 3e). In contrast to the unobservable CD signal of the achiral H_4TPPS_4 monomer, the addition of chiral tartaric acid induces a very intense, reproducible CD signal in the J-band region; positive/negative and negative/positive CD spectral patterns are induced by the addition of L- and D-tartaric acids, respectively (Fig. 3f). Therefore, the enantioselective formation of J-aggregates of H_4TPPS_4 could be controlled. Density functional theory (DFT) calculations (B3LYP/6-31G*) indicate that the porphyrin units interact to form left-handed helical, planar, or right-handed helical structures (Fig. 3b–d). The right- or left-handed helical structure is preferably formed when the pyrrole protons in the upper and lower porphyrin interact with the sulfonic acid functional groups in the lower and upper porphyrin, respectively. This structure is preferred because the Coulomb interactions between the sulfonic acid groups and the pyrrole protons are more favourable owing to reduced steric hindrance. The planar structure is generated when the pyrrole protons involved in the interaction are located on the right- and left-hand sides of the upper and lower porphyrins, respectively. For a chiral tetramer adopting the optimised helical and planar structures, the experimentally obtained dispersion-type CD spectral pattern can be reproduced by calculations based on the exciton chirality method. The MCD spectrum of the H_4TPPS_4 monomer shows an intense, dispersion-type signal that corresponds to the Soret band, which is labelled the Faraday A-term (Fig. 3g). This behaviour is a reflection of the orbital angular momentum that derives from the large aromatic π-conjugated system of the porphyrin in addition to the degeneracy of the Soret band. In the case of the chiral J-aggregates of H_4TPPS_4, an intense, integral-type MCD signal (Faraday B-term) is observed for the J-band (490 nm), indicative of nondegeneracy.

Because the very intense CD signal and the MCD signal are simultaneously observed in the J-band region of the chiral J-aggregates of H_4TPPS_4, MChD signals were evaluated in the J-band region by measuring the difference in absorbance when the externally applied magnetic field was parallel and antiparallel to the direction of light propagation (Fig. 3h). When the J-aggregates are prepared by adding L-tartaric acid, a sharp, positive MChD signal is observed at 490 nm; the MChD signal of the J-aggregates prepared using D-tartaric acid is observed at the same wavelength, but the sign is negative (Fig. 3h). The peak position (490 nm) of the MChD spectrum is identical to that of the spectrum obtained from the product of the CD and MCD spectra. This finding is consistent with previous reports,[1,2,6] and thus, the presence of MChD in organic compounds was demonstrated for the first time.

Magneto-chiral dichroism based on π–π* transitions

In addition to the MChD observed for chiral J-aggregates of water-soluble tetraarylporphyrins, it is important to confirm the presence of MChD for the π–π* transitions by demonstrating its existence in other systems. The observation of MChD is important, not only for clarification of asymmetry observed in biological systems, but also for the development of novel applications, such as asymmetric synthetic methods and magneto-optical devices. Ishii and co-workers demonstrated the second example of MChD for π–π* transitions using chiral J-aggregates of zinc(II) chlorins (ZnChls, Fig. 4a and b).[11] This supramolecular system is a model compound for the light-harvesting antennas in green photosynthetic bacteria (*i.e.*, chlorosomes), which are formed through the self-assembly of a large number of bacteriochlorophyll molecules without the assistance of proteins. In this system, the Zn^{2+} ion was employed as the central metal ion instead of the Mg^{2+} ion (as found in Nature), because Zn chlorins are more stable than Mg chlorins. In order to acquire an intense CD signal based on exciton chirality, a hydrophilic tetraoxyethylene chain was incorporated into ZnChl. The J-aggregates of ZnChls were prepared by diluting a methanol solution of ZnChl with a 99-fold volume of water.

The UV-vis, MCD, and CD spectra in the Q band region of the ZnChl monomer and chiral J-aggregates of ZnChls are shown in Fig. 4. The UV-vis spectrum of the ZnChl monomer shows typical Q absorption bands for metallochlorins at 658, 611, and 581 nm, which are attributed to the $Q_y(0,0)$, $Q_y(1,0)$, and $Q_x(0,0)$ bands, respectively. In the MCD spectrum of the ZnChl monomer, these bands show intense integral-type MCD signals (the Faraday B-term), which indicate the nondegeneracy of the excited states. In the UV-vis spectrum of the chiral J-aggregates of ZnChls, the Q_y band showed a remarkable bathochromic shift to 729 nm due to the exciton interaction between ZnChl constituents, whereas the shift of the Q_x band is very small. This indicates that the long axis of the J-aggregates is nearly parallel to the transition dipole moment of the Q_y band. Thus, J-aggregation increases the energy separation between the Q_y and Q_x bands (monomer, 2120 cm^{-1}; J-aggregates, 3510 cm^{-1}). This is consistent with the relatively weak MCD intensity of the Q_y band of the J-aggregates (one-third weaker than that of the corresponding monomer) because the Faraday B-term is inversely proportional to the energy separation. The full width at half maximum of the J-band is very narrow (280 cm^{-1}), which indicates that the ZnChl chromophores form highly ordered J-aggregates. DFT calculations (B3LYP/6-31G*) for the ZnChl dimer indicate that the 3^1-methoxy group of one ZnChl coordinates to the Zn^{2+} ion of the other ZnChl. In addition, the transition electric dipole moments of the Q_y band are calculated to be almost parallel to the long axis of the dimer, which is consistent with the observed J-band. The chiral J-aggregates of ZnChls show an intense, inverse sigmoidal-shaped CD signal in the J-band region (red line in Fig. 4e), whereas the CD signals of the corresponding monomer that are attributed to the chiral centre (Fig. 4a, positions 17 and 18) are very weak (black line in Fig. 4e). The inverse sigmoidal-shaped CD spectral pattern originates from exciton chirality owing to the twisted configuration between the chromophores with a large transition electric dipole moment; this configuration is consistent with the optimised structure

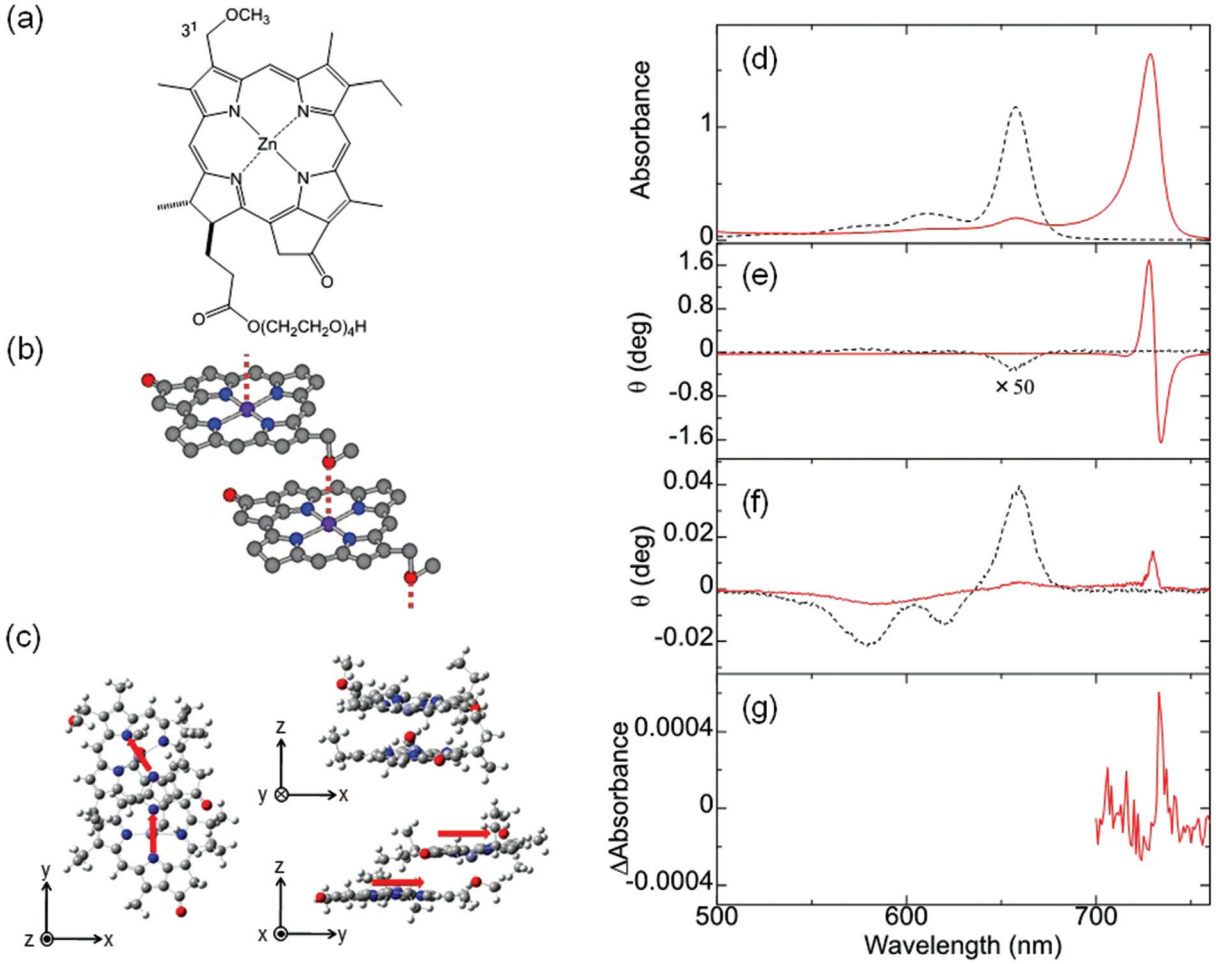

Fig. 4 ZnChl, a model compound of light-harvesting antenna. Molecular structures of (a) ZnChl, (b) J-aggregates of ZnChls, and (c) the optimised ZnChl dimer. The (d) UV-vis, (e) MCD, (f) CD, and (g) MChD spectra of the chiral J-aggregates of ZnChls. The red arrows indicate the transition electric dipole moments of the ZnChl constituents at the Q_y band. Reproduced from ref. 11 with permission from The Royal Society of Chemistry.

(Fig. 4c). A positive MChD signal at 733 nm (Fig. 4g) is identical to that of the spectrum obtained from the product of the CD and MCD spectra of chiral J-aggregates of ZnChls, which is similar to that observed for the chiral J-aggregates of H_4TPPS_4. Further, the MChD signal for the chiral J-aggregates of ZnChls was observed at 5 T using a MChD measurement with a pulsed electromagnet (Fig. 5).[43] From the viewpoint of photosynthesis, observation of MChD in the light-harvesting antenna model indicates the possibility of MChD occurring during the light-harvesting process. This is an intriguing twist to our understanding of photosynthesis, as novel magnetic field effects may play a nuanced yet important role in light-harvesting in Nature.[44–51] Jiang and co-workers reported the third example of MChD for π–π* transitions using chiral rare earth triple-decker complexes comprising one phthalocyanine and two porphyrin ligands, which exhibit single-molecule magnet (SMM) behaviour.[12] These MChD observations based on the π–π* transition emphasise that on the basis of π electronic properties (*e.g.*, orbital angular momentum and exciton chirality), MChD should be

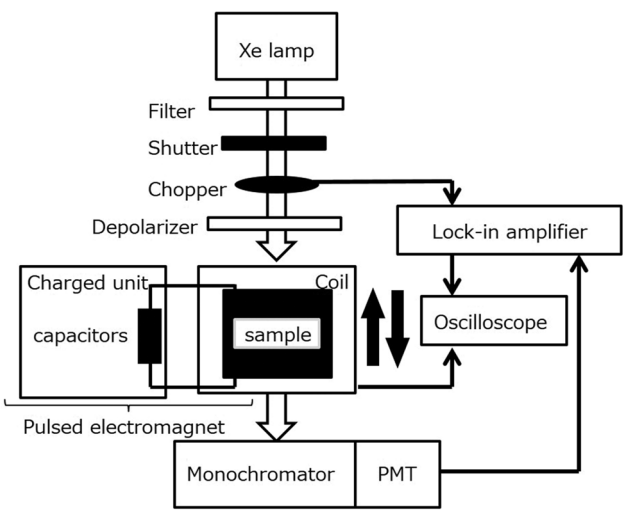

Fig. 5 Block diagram of a typical pulsed magneto-chiral dichroism measurement system. Reproduced from ref. 43 with permission from Elsevier.

observed in the aggregates of conventional organic aromatic compounds.

Theoretical explanations for the magneto-chiral dichroism of aromatic π-conjugated systems

Based on eqn (1), the MChD intensity is dependent on four matrix elements: (1) the transition electric dipole moments between the *a* and *n* (or *m*) states, (2) the transition magnetic dipole moments between the *a* and *n* (or *m*) states, (3) the transition electric quadrupole moments between the *a* and *n* (or *m*) states, and (4) the magnetic dipole moments between the *n* and *m* states.

The MCD intensity is related to the intensity of MChD. The magnetic dipole moments between the *n* and *m* states correspond to the orbital angular momentum between the *n* and *m* states as evaluated by MCD. Based on the Zeeman effects, both MCD and MChD are intensified by the d (or f) orbital-based degeneracy and angular momentum of metals. In the case of organic aromatic compounds, however, m_l, which is related to the orbital angular momentum, increases with increasing π-conjugated systems.[37,38] If we consider diamagnetic aromatic compounds, the MCD intensity is proportional to the orbital angular momentum between the excited states. The magnitude of the orbital angular momentum therefore corresponds to the magnetic quantum number, m_l. Similar to atomic orbitals, π molecular orbitals of aromatic π-conjugated systems are quantised by m_l (Fig. 6a). Although the maximum m_l values of d orbitals (m_l = 0, ±1, ±2) and f orbitals (m_l = 0, ±1, ±2, ±3) are 2 and 3, respectively, those of π molecular orbitals increase as the size of the π-conjugated system increases.[37,38] For example, the m_l values of the HOMO and LUMO of $C_{16}H_{16}^{2-}$, which is a simple model of a porphyrin analogue, are ±4 and ±5, respectively. In this case, the orbital angular momentum of the excited states corresponds to M_L = ±1 or ±9 (Fig. 6b). Thus, in spite of weak absorbance, strong MCD signals are observed for the absorption band with M_L = ±9 (Fig. 6c and d). Therefore, large aromatic π-conjugated systems, such as porphyrinic compounds, are appropriate for intensifying not only MCD but also MChD.

The CD intensity is also correlated with the MChD intensity. The CD intensity is a function of an imaginary part of the cross product of the transition electric dipole moment and the transition magnetic dipole moment.[39,40] Because the electric dipole moment and the magnetic dipole moment are associated with linear and rotational electronic motions, respectively, the requisite conditions for coexistence are severe. Therefore, CD transitions should be very weak in conventional systems, yet contrary to the previous explanation, CD transitions can actually be very intense due to exciton chirality; enhancement of CD intensity induced by exciton chirality originates from the approximation from the transition magnetic dipole moment to the transition electric dipole moments of the constituting chromophores. For example, when a dimer is formed by two chromophores (Fig. 7a), low and high exciton states are generated due to the exciton interaction between the chromo-

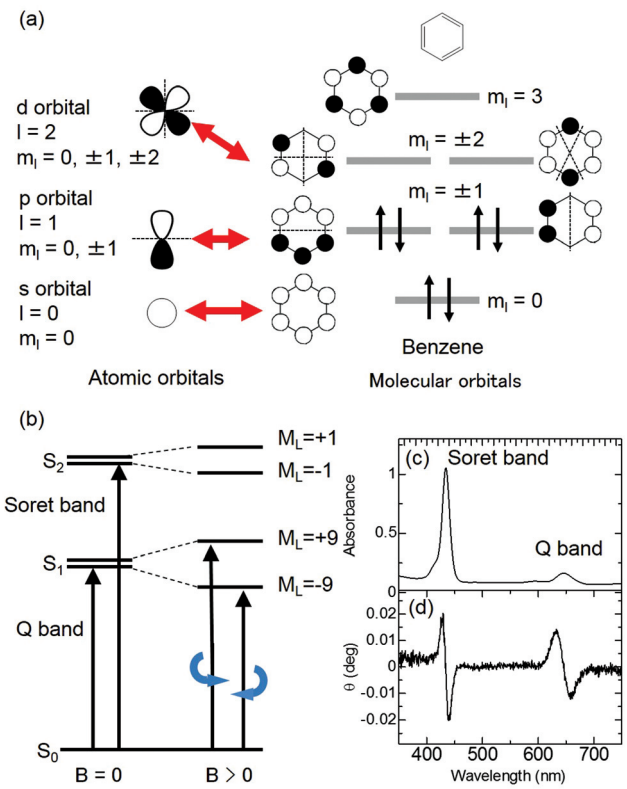

Fig. 6 Representative explanation for the intensification of MCD by the orbital angular momentum of π-conjugated systems. (a) The relationship between atomic orbitals and molecular orbitals. (b) The energy state diagram of absorption (left) and MCD (right) for π-conjugated systems. (c) UV-vis and (d) MCD spectra of the protonated form of *meso*-tetrakis (4-sulfonatophenyl)porphine (H_4TPPS_4). Reproduced from ref. 14 with permission from OSA Publishing.

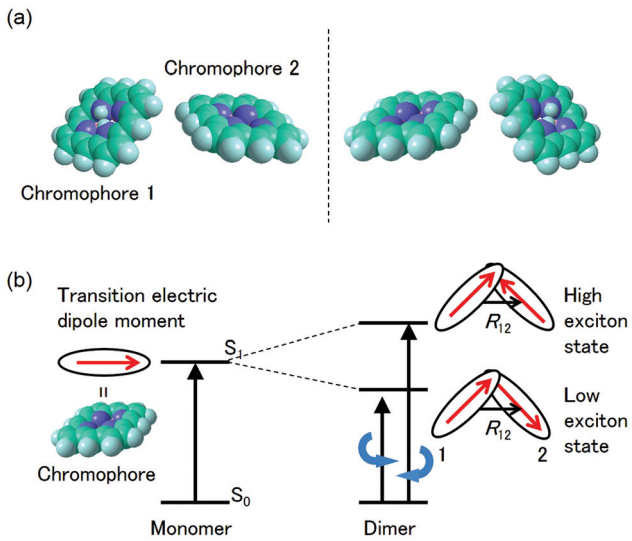

Fig. 7 Explanation of exciton chirality using a porphyrin dimer. (a) Molecular structures of a pair of enantiomers. (b) The energy state diagram of the CD transitions for one of the enantiomers.

phores (Fig. 7b). When the transition electric dipole moments of the chromophores are twisted in a chiral dimer, the transition magnetic moment is approximated by the vector products of transition electric dipole moments and position vectors according to:

$$\sum_{p=1}^{2} m^{(p)} = \sum_{p=1}^{2} \left(-\frac{\omega_{na}{}^{(p)}}{2} r_0{}^{(p)} \times \mu^{(p)} \right) \quad (19)$$

where $r_0{}^{(p)}$ and $\mu^{(p)}$ are the position vector and the transition electric dipole moment for a p unit, respectively. In addition, the intrinsic magnetic dipole moment can be neglected since it is sufficiently small for the π–π* transition. Thus, strong CD intensities can be observed for a system such as an aromatic compound with a very intense transition electric dipole moment. This phenomenon is called exciton chirality.[38,39] Because the CD sign of the low and high exciton states is opposite, dispersion-type CD spectra are observed for conventional chiral dimers. Furthermore, the absolute configuration of chromophores in the dimer can be determined from the analysis of the CD spectra. Therefore, when aromatic compounds with large transition electric dipole moments (*e.g.*, porphyrins and porphyrin analogues) are twisted, as is the case in the chiral J-aggregates of porphyrins, both MChD and CD are strengthened.

Finally, the transition electric quadrupole moments between the a and n (or m) states can also be related to exciton chirality. Based on the exciton chirality, the quadrupole moment can be rewritten using the transition electric dipole moments of the constituting chromophores as follows:[3,40]

$$\sum_{p=1}^{2} \Theta_{\alpha\beta}^{(p)} = -\frac{3}{2} \sum_{p=1}^{2} (r_\beta^{(p)} \mu_\alpha^{(p)} + r_\alpha^{(p)} \mu_\beta^{(p)}) \quad (20)$$

and this is negligible since it is also sufficiently small for the π–π* transition. Using these equations, MChD based on exciton chirality can thus be reproduced from the wavefunctions of the exciton states.

Photoresolution based on magneto-chiral dichroism

It has been well established that circularly polarised light (CPL) can induce enantioselective photochemical reactions (photoresolution) on the basis of CD (*i.e.*, differences in absorption coefficients between two enantiomers from CPL).[52–54] The enantiomeric excess (ee) owing to the CPL induced photoresolution is given by $g_{CD}/2$. The ee value would be small even from pure CPL from synchrotron radiation because the g_{CD} values of organic compounds are small. On the other hand, after the theoretical prediction by Barron,[55,56] Rikken and Raupach studied MChD-based photochemistry that results in enantioselective reactions.[57] Here, based on the magnetic field effect of the MChD mechanism, an observable photoresolution can be expected even though unpolarised light was used. A thermally racemic mixture of Δ- and Λ-chromium(III) tris(oxalato) ($[Cr(ox)_3]^{3-}$) was employed. The photoresolution of this complex has been extensively studied with CPL;[52] one enantiomer should be preferably formed under irradiation with CPL, which is selectively absorbed by the other enantiomer, since ligand dissociation is accelerated by photoexcitation. Thus, this photoresolution is much faster than thermal racemisation. Because one enantiomer selectively absorbs unpolarised light under a magnetic field that is parallel (or antiparallel) to the direction of light propagation, an ee value is obtained for the racemic mixture of Δ- and Λ-$[Cr(ox)_3]^{3-}$ complexes owing to magneto-chiral anisotropy.

Similar to photoresolution with CPL, the ee owing to MChD is given by $g_{MChD}/2$. For the spin-forbidden transition from the ground state ($^4A_{2g}$) to the excited state (^2E_g) of $[Cr(ox)_3]^{3-}$, both g_{CD} and g_{MCD} values are very large; therefore, a large g_{MChD} value can be expected. Fig. 8b shows the ee due to MChD, where the $^4A_{2g} \rightarrow {}^2E_g$ transition was selectively excited. When the magnetic field direction was parallel to the direction of light propagation, the ee/B value was 1.0×10^{-5} T^{-1}. On the other hand, when the magnetic field direction was perpendicular to the direction of light propagation, no significant ee was observed. These results are in agreement with the properties of MChD, thus demonstrating photoresolution based on MChD.

Fig. 8c shows the excitation wavelength dependence of the ee under 7.5 T, in which a correlation between the dispersion-type spectrum and A-term is observed. Since the ee due to MChD is approximated as $(g_{CD} \times g_{MCD})/2$ based on eqn (18), the g_{MCD}/B (1.2×10^{-3} T^{-1}) and g_{CD} (2.2×10^{-3}) values at

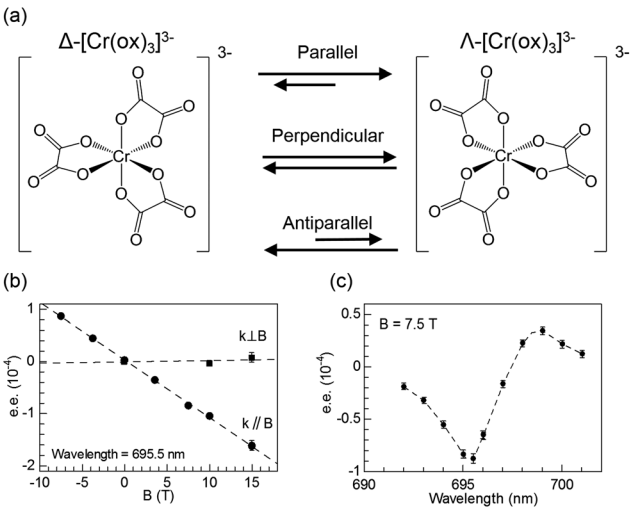

Fig. 8 (a) Equilibrium between two enantiomers of $[Cr(ox)_3]^{3-}$, (b) enantiomeric excess of $[Cr(ox)_3]^{3-}$ obtained after irradiation with unpolarised light (695.5 nm; either parallel ($k \| B$) or perpendicular ($k \perp B$) to the magnetic field direction) as a function of the magnetic field, and (c) enantiomeric excess of $[Cr(ox)_3]^{3-}$ obtained after irradiation with unpolarised light as a function of the irradiation wavelength (magnetic field of 7.5 T is parallel to the direction of light propagation). Reproduced from ref. 57 with permission from Springer Nature.

701 nm were used to determine an ee/B value of 1.3×10^{-6} T^{-1}, which is close to the observed ee/B value (1.7×10^{-6} T^{-1}). In addition to pure MChD, cascaded MChD should also be present. The ee due to cascaded MChD is expressed as follows:

$$ee_{casc} = \frac{\ln T}{8} g_{MCD} \times g_{CD} \quad (21)$$

Here, T denotes the transmittance. Using eqn (21), the ee_{casc}/B value was calculated as 5×10^{-7} T^{-1} at 701 nm, which is an order of magnitude smaller than the observed ee/B value of 1.7×10^{-6} T^{-1}. Thus, the observed ee resulting from the photochemical reactions of $[Cr(ox)_3]^{3-}$ predominantly originates from pure MChD. The observed ee/B value is consistent with the $g_{MChD}/2$ value, which was determined for pure enantiomers.

Harnessing the effects of MChD, Xu *et al.* experimentally demonstrated the enantioselective photopolymerisation of a diacetylene (DA) derivative in the liquid crystal (LC) phase, which was previously achieved with irradiation of CPL.[58] Photopolymerisation of DA units in the LC phase was performed using linearly polarised light (LPL) under different magnetic field conditions (zero magnetic field, and magnetic field either perpendicular or parallel to the beam of LPL). After polymerisation, a typical intense absorption maximum was observed at ~640 and 580 nm, indicating the formation of polymeric DA (PDA) chains. When the magnetic field is parallel or antiparallel to the direction of LPL irradiation, an intense Cotton effect of the CD signals corresponding to the absorption bands of the PDA backbone appear at 550 and 670 nm with a crossover at 640 nm, indicating the helical formation of PDA chains. In contrast, when zero magnetic field or a magnetic field perpendicular to the beam of LPL is used, the observed CD signal is weak. Thus, MChD was successfully utilised to realise the enantioselective polymerisation of DA units by the application of LPL and a magnetic field either parallel or antiparallel to the direction of LPL irradiation. Moreover, the prepared helical PDA assemblies could be used to enantioselectively recognise D- or L-lysine.

Homochirality of life

From a chemical viewpoint, three plausible candidates, *i.e.*, (1) the rotational motion of the Earth (the Coriolis force), (2) CPL-induced asymmetric photochemical reactions, and (3) MChD-induced asymmetric photochemical reactions, have been proposed to explain the origins of the homochirality of life (Fig. 9).[15,16] Discovery of an excess of L-amino acids in the Murchison meteorite has attracted considerable attention with respect to their relationship with the homochirality of life,[59] prompting more questions that require explanations to understand the organic asymmetric reactions that occur in the universe. Asymmetric reactions seem to likely occur in regions relatively close to neutron stars due to the presence of both enormous magnetic fields (10^8–10^{12} T) and synchrotron radiation.[60,61] Although the pure CPL of synchrotron radiation can induce stereoselectivity in photochemical reactions, the ee value should be small since the g_{CD} values of conventional organic compounds are rather small. On the other hand, the g_{MChD} value is proportional to the magnetic field, thus the ee value due to MChD should be high under the influence of the enormous magnetic fields near neutron stars. For example, MChD-based photochemical reactions of aromatic amino acids may contribute to the asymmetric reactions in the universe because aromatic amino acids exhibit both CD and MCD. Furthermore, intense MChD observed in metal compounds suggests that the MChD of organic compounds may be observed in the X-ray or UV region, which could also potentially contribute to organic asymmetric reactions in the universe. Polyaromatic hydrocarbons (PAHs) are also found in the Murchison meteorite and they are the most abundant organic molecules in the universe (encompassing 20% of total cosmic carbon).[62–64] Even in the aggregates of conventional organic aromatic compounds, such as PAHs, MChD can occur based

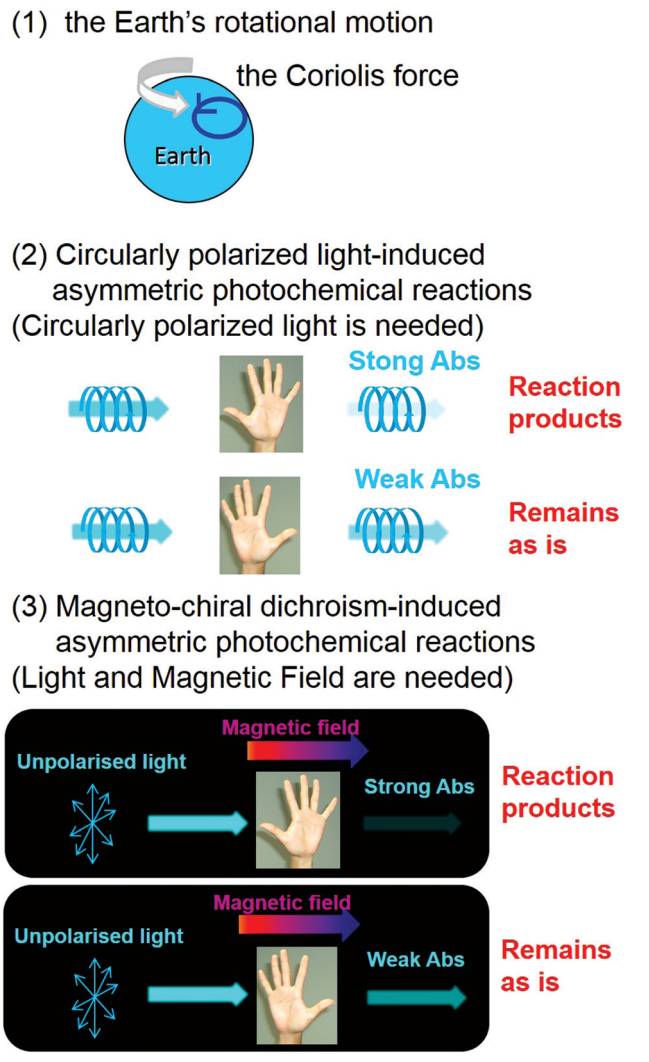

Fig. 9 Plausible candidates for explaining the homochirality of life:[15,16] (1) the rotational motion of the Earth (the Coriolis force), (2) CPL-induced asymmetric photochemical reactions, and (3) MChD-induced asymmetric photochemical reactions.

on the previous observations. Furthermore, the MChD-based photoresolution in these systems is highly expected because of the experimental demonstration in the enantioselective photopolymerisation reactions of DA derivatives. Thus, because regions that have a very strong magnetic field exist in the universe, such as those within the vicinity of neutron stars (10^8 T–10^{12} T),[60] the MChD of PAH aggregates could potentially lead to asymmetric photochemical reactions that introduce a small bias in chirality. Thus, the future development of MChD studies will be concerned not only with the development of magneto-optical devices and asymmetric photochemical reactions, but also for providing insight into the homochirality of life.

Conclusions

In this perspective, the progress of MChD studies has been reviewed, especially focusing on organic compounds. In addition to the MChD enhancements observed in metal complexes, MChD studies of organic compounds have progressed from aromatic π-conjugated systems to enantioselective photopolymerisation reactions. From the viewpoint of the magnetic field effect, the radical pair mechanism has been investigated in various photochemical reactions,[65–70] including photosynthesis.[44–51] MChD observations on the artificial model of a photosynthetic light-harvesting antenna are attractive in terms of the novel magnetic field effect in photosynthesis, which may explain unsolved questions related to the magnetic field effects in biological systems. Based on these studies, MChD should not only be useful for asymmetric synthetic methods, but is also currently one of the plausible candidates for explaining the origins of the homochirality of life.

Conflicts of interest

There are no conflicts to declare.

Acknowledgements

This work was supported by the JSPS KAKENHI JP17H06375. Y. K. acknowledges financial support from the JSPS KAKENHI JP19H04556. S. H. acknowledges financial support from the Yokohama Academic Foundation (1971000033) and the JSPS KAKENHI JP19K23634.

Notes and references

1 G. Wagnière and A. Meier, *Chem. Phys. Lett.*, 1982, **93**, 78.
2 L. D. Barron and J. Vrbancich, *Mol. Phys.*, 1984, **51**, 715.
3 L. D. Barron, *Molecular Light Scattering and Optical Activity*, Cambridge University press, Cambridge, 2nd edn, 2007.
4 G. L. J. A. Rikken and E. Raupach, *Nature*, 1997, **390**, 493.
5 G. L. J. A. Rikken and E. Raupach, *Phys. Rev. E: Stat. Phys., Plasmas, Fluids, Relat. Interdiscip. Top.*, 1998, **58**, 5081.
6 N. B. Baranova and B. Ya. Zel'dovich, *Mol. Phys.*, 1979, **38**, 1085.
7 E. Raupach, G. L. J. A. Rikken, C. Train and B. Malézieux, *Chem. Phys.*, 2000, **261**, 373.
8 C. Train, R. Gheorghe, V. Krstic, L.-M. Chamoreau, N. S. Ovanesyan, G. L. J. A. Rikken, M. Gruselle and M. Verdaguer, *Nat. Mater.*, 2008, **7**, 729.
9 M. Saito, K. Ishikawa, K. Taniguchi and T. Arima, *Phys. Rev. Lett.*, 2008, **101**, 117402–117401.
10 Y. Kitagawa, H. Segawa and K. Ishii, *Angew. Chem., Int. Ed.*, 2011, **50**, 9133.
11 Y. Kitagawa, T. Miyatake and K. Ishii, *Chem. Commun.*, 2012, **48**, 5091.
12 K. Wang, S. Zeng, H. Wang, J. Dou and J. Jiang, *Inorg. Chem. Front.*, 2014, **1**, 167.
13 Y. Kitagawa and K. Ishii, in *Advances in Multi-Photon processes and Spectroscopy: Volume 22*, ed. S. H. Lin, A. A. Villaeys and Y. Fujimura, World Scientific, Singapore, 2014.
14 S. Hattori and K. Ishii, *Opt. Mater. Express*, 2014, **4**, 2423.
15 G. H. Wagnière, *On Chirality and the Universal Asymmetry: Reflections on Image and Mirror*, VHCA, Wiley-VCH, Weinheim, 2007.
16 A. Guijarro and M. Yus, *The Origin of Chirality in the Molecules of Life*, RSC Publishing, Cambridge, 2009.
17 C. Görller-Walrand and J. Godemont, *J. Chem. Phys.*, 1997, **67**, 3655.
18 K. Stadnicka, A. M. Glazer and M. Koralewski, *Acta Crystallogr., Sect. B: Struct. Sci.*, 1987, **B43**, 319.
19 A. J. McCaffery, P. J. Stephens and P. N. Schatz, *Inorg. Chem.*, 1967, **6**, 1614.
20 G. Kopnov and G. L. J. A. Rikken, *Rev. Sci. Instrum.*, 2014, **85**, 053106.
21 N. Nakagawa, N. Abe, S. Toyoda, S. Kimura, J. Zaccaro, I. Gautier-Luneau, D. Luneau, Y. Kousaka, A. Sera, M. Sera, K. Inoue, J. Akimitsu, Y. Tokunaga and T. Arima, *Phys. Rev. B*, 2017, **96**, 121102.
22 S. Eslami, J. G. Gibbs, Y. Rechkemmer, J. van Slageren, M. Alarcón-Correa, T.-C. Lee, A. G. Mark, G. L. J. A. Rikken and P. Fischer, *ACS Photonics*, 2014, **1**, 1231.
23 K. Taniguchi, M. Nishio, S. Kishiue, P.-J. Huang, S. Kimura and H. Miyasaka, *Phys. Rev. Mater.*, 2019, **3**, 045202.
24 K. Taniguchi, S. Kishiue, S. Kimura and H. Miyasaka, *J. Phys. Soc. Jpn.*, 2019, **88**, 093708.
25 V. Yannopapas and A. G. Vanakaras, *ACS Photonics*, 2015, **2**, 1030.
26 V. Yannopapas, *Solid State Commun.*, 2015, **217**, 47.
27 M. Ceolín, S. Goberna-Ferrón and J. R. Galán-Mascarós, *Adv. Mater.*, 2012, **24**, 3120.
28 R. Sessoli, M.-E. Boulon, A. Caneschi, M. Mannini, L. Poggini, F. Wilhelm and A. Rogalev, *Nat. Phys.*, 2015, **11**, 69.
29 S. Bordács, I. Kézsmárki, D. Szaller, L. Demkó, N. Kida, H. Murakawa, Y. Onose, R. Shimano, T. Rõõm, U. Nagel, S. Miyahara, N. Furukawa and Y. Tokura, *Nat. Phys.*, 2012, **8**, 734–738.

30 S. Kibayashi, Y. Takahashi, S. Seki and Y. Tokura, *Nat. Commun.*, 2014, **5**, 4583.
31 H. Narita, Y. Tokunaga, A. Kikkawa, Y. Taguchi, Y. Tokura and Y. Takahashi, *Phys. Rev. B*, 2016, **94**, 094433.
32 Y. Takahashi, S. Kibayashi, Y. Kaneko and Y. Tokura, *Phys. Rev. B*, 2016, **93**, 180404.
33 Y. Okamura, F. Kagawa, S. Seki, M. Kubota, M. Kawasaki and Y. Tokura, *Phys. Rev. Lett.*, 2015, **114**, 197202.
34 S. Tomita, K. Sawada, A. Porokhnyuk and T. Ueda, *Phys. Rev. Lett.*, 2014, **113**, 235501.
35 S. Tomita, H. Kurosawa, K. Sawada and T. Ueda, *Phys. Rev. B*, 2017, **95**, 085402.
36 Y. Nii, R. Sasaki, Y. Iguchi and Y. Onose, *J. Phys. Soc. Jpn.*, 2017, **86**, 024707.
37 K. Ishii, *Jasco Rep.*, 2013, **55**, 1.
38 J. Mack, M. J. Stillman and N. Kobayashi, *Coord. Chem. Rev.*, 2007, **251**, 429.
39 M. Nakazaki, *Introduction to theory of optical rotation*, Baifukan, Tokyo, 1973.
40 N. Harada and K. Nakanishi, *Cirucular Dichroic Spectroscopy-Exciton Coupling in Organic Stereochemistry*, Tokyo Kagaku Dojin, Tokyo, 1982.
41 O. Ohno, Y. Kaizu and H. Kobayashi, *J. Chem. Phys.*, 1993, **99**, 4128.
42 J. M. Ribó, J. Crusats, J.-A. Farrera and M. L. Valero, *J. Chem. Soc., Chem. Commun.*, 1994, 681.
43 S. Hattori, Y. Yamamoto, T. Miyatake and K. Ishii, *Chem. Phys. Lett.*, 2017, **674**, 38.
44 Y. Tanimoto, H. Hayashi, S. Nagakura, H. Sakuragi and K. Tokumaru, *Chem. Phys. Lett.*, 1976, **41**, 267.
45 K. Schulten, H. Staerk, A. Weller, H.-J. Werner and B. Nickel, *Z. Phys. Chem. Neue Folge*, 1976, **101**, 371.
46 N. Hata, *Chem. Lett.*, 1976, **5**, 547.
47 Y. Sakaguchi, H. Hayashi and S. Nagakura, *Bull. Chem. Soc. Jpn.*, 1980, **53**, 39.
48 H. Hayashi and S. Nagakura, *Bull. Chem. Soc. Jpn.*, 1984, **57**, 322.
49 Y. Sakaguchi and H. Hayashi, *J. Phys. Chem.*, 1984, **88**, 1437.
50 U. E. Steiner and T. Ulrich, *Chem. Rev.*, 1989, **89**, 51.
51 J. F. Rabek, *Photochemistry and Photophysics vol. I*, CRC Press, US, 1990.
52 K. L. Stevenson and J. F. Verdieck, *Mol. Photochem.*, 1969, **1**, 271.
53 H. Rau, *Chem. Rev.*, 1983, **83**, 535.
54 Y. Inoue, *Chem. Rev.*, 1992, **92**, 741.
55 L. D. Barron, *J. Am. Chem. Soc.*, 1986, **108**, 5539.
56 L. D. Barron, *Rend. Fis. Acc. Lincei*, 2013, **24**, 179.
57 G. L. J. A. Rikken and E. Raupach, *Nature*, 2000, **405**, 932.
58 Y. Xu, G. Yang, H. Xia, G. Zou, Q. Zhang and J. Gao, *Nat. Commun.*, 2014, **5**, 5050.
59 M. H. Engel and B. Nagy, *Nature*, 1982, **296**, 837.
60 A. G. Lyne, *Nature*, 1984, **308**, 605.
61 W. A. Bonner and E. Rubenstein, *Biosystems*, 1987, **20**, 99.
62 E. Dwek, R. G. Arendt, D. J. Fixsen, T. J. Sodroski, N. Odegard, J. L. Weiland, W. T. Reach, M. G. Hauser, T. Kelsall, S. H. Moseley, R. F. Silverberg, R. A. Shafer, J. Ballester, D. Bazell and R. Isaacman, *Astrophys. J.*, 1997, **475**, 565.
63 J. H. Hahn, R. Zenobi, J. L. Bada and R. N. Zare, *Science*, 1988, **239**, 1523.
64 M. P. Bernstein, S. A. Sandford, L. J. Allamandola, J. S. Gillette, S. J. Clemett and R. N. Zare, *Science*, 1999, **283**, 1135.
65 F. J. Adrian, *J. Chem. Phys.*, 1971, **54**, 3918.
66 J. B. Pedersen and J. H. Freed, *J. Chem. Phys.*, 1973, **58**, 2746.
67 J. B. Pedersen and J. H. Freed, *J. Chem. Phys.*, 1973, **59**, 2869.
68 F. J. Adrian and L. Monchick, *J. Chem. Phys.*, 1979, **71**, 2600.
69 F. J. Adrian and L. Monchick, *J. Chem. Phys.*, 1980, **72**, 5786.
70 A. Marais, I. Sinayskiy, F. Petruccione and R. van Grondelle, *Sci. Rep.*, 2015, **5**, 8720.